

Supplementary Materials for
**Green biomass: Impact of high-adhesion and well-dispersed
binders on the sodium storage performance and interfacial
interaction of hard carbon anodes**

Jiaqi Jiao ^a, Conghua Yi ^{a,*}, Xueqing Qiu ^{b,*}, Dongjie Yang ^a, Fangbao Fu ^b, Weifeng Liu ^a

^a School of Chemistry and Chemical Engineering, South China University of Technology,
381Wushan Road, Tianhe District, Guangzhou, 510641, China.

^b School of Chemical Engineering and Light Industry, Guangdong Provincial Key Laboratory
of Plant Resources Biorefinery, Guangdong University of Technology, Waihuan Xi Road 100,
Guangzhou, 510006, China.

***Corresponding Author**

E-mail: chyi@scut.edu.cn (C.Y.) and qxq@gdut.edu.cn (X.Q.).

Materials and general methods

Preparation of binders

The sodium lignosulfonate (from Chempack Company, Russia) and CMC (viscosity 1500-3000 mPa s, degree of substitution 0.8-1.2, Canrd) were added to a beaker at room temperature in various mass ratios (7:1, 5:1, 1:1, and 2:1). The solution was then brought to the proper concentration by adding water and stirred with a magnetic stirrer at 500 rpm for 12 hours, that assisted in dissolving the CMC and LS. The resulting binders were designated C7L1, C5L1, C1L1, and C1L2.

Preparation of hard carbon anodes

The working electrodes were formed by mixing 80 wt% commercial hard carbon (purchased from Kureha Chemical, Japan), 10 wt% superconducting carbon (purchased from Shenzhen Jingle Nano Technology Co., Ltd.), and 10 wt% binders. The binders used were PVDF, CMC, and CMC/LS(PVDF was purchased from Canrd). PVDF needed to be dissolved in N-methylpyrrolidone (NMP, purchased from Canrd) , CMC and CMC/LS in deionized water. The solvent (NMP or deionized water) was added to the solid powder and mixed by a Semi-circular arc planetary ball mill (PBM-0.4A, Xinhua Hydrogen Energy Technology Co.).After homogeneous mixing, the slurry was coated onto the copper foil at a thickness of 100-200 μm and vacuum-dried at 110 °C for 12 h. Subsequently, each electrode film was cut into 12 mm circles to obtain working electrodes named HC-PVDF, HC-CMC, HC-C7L1, HC-C5L1, HC-C1L1, and HC-C1L2, respectively. The mass loading of the active material was about 1.0-1.5 mg cm^{-2} .

Material characterization

Ultra-high resolution field emission electron microscopy (Horiba, FE-SEM, SU8200) was used to

observe the surface morphology and microstructure of each electrode before cycling, after 3 and 100 cycles. The Raman spectra of the materials were detected by a laser confocal microscopy Raman spectrometer (Horiba Jobin Yvon), nano-indentation experiments were carried out on a nanoindentation machine (Bruker/TI 980) and a constant load of 1 mN was applied during the experiments. The composition of the SEI layer after 3 cycles at 0.05 A g⁻¹ was studied by depth analysis on the electrodes by XPS (Thermo Scientific K-Alpha), indicated etching depths were calculated based on the Ar etching time and rate (0.2 nm s⁻¹). The morphology and microstructure of the SEI layer of the HC electrodes after disassembled batteries were investigated with a Talos F200S transmission electron microscope (TEM, Thermo Fisher Scientific, USA). The 180° peel test of the pole piece was performed by a universal tensile machine (AG-Xplus HS). A paste of size 25 mm wide and 40 mm long was coated on the copper foil and peeled off 3M 810 transparent tape at a constant rate of 60 mm min⁻¹. A laser particle size and zeta potential analyzer (ZetaPALS, Brookhaven, USA) were used to test the particle size and zeta potential of the slurry, all test temperatures were 25°C. The amount of binder effectively adsorbed on the surface of the hard carbon particles was determined by centrifuging the hard carbon suspension at 10000 rpm and separating the hard carbon particles that were firmly bonded to the binder. After centrifugation, the hard carbon particles were dried overnight in an infrared oven at 50°C and the total amount of the binder was measured by thermogravimetric analysis (TG, Germany-NETZSCH TG 209F3).

Electrochemical testing

The CR2032 coin cell was assembled in a glove box with 1 M NaPF6 DME (Ethylene Glycol Dimethyl Ether) as the electrolyte (Dodo Chemical Reagents). A fiberglass (Whatman) diaphragm was used, and a sodium sheet (purchased from Shanghai Changgao New Material Technology Co.)

was used as the counter electrode. The batteries were charged and discharged by a multi-channel battery test system (Shenzhen Neware Electronics Co., Ltd., Shenzhen, China) at 0.01 to 3.00 V (vs. Na^+/Na) and different current densities, and the assembled coin cell was subjected to CV and EIS tests on a Bio-Logic electrochemical workstation (BioLogic MPG₂), 0.01 to 3.00 V (vs. Na^+/Na). The cells were allowed to rest at open-circuit voltage (OCV) for 12 hours before electrochemical testing.

Theoretical simulations

Non-covalent interactions (NCIs) were analyzed using the independent gradient model based on the Hirshfeld partition (IGMH) method via the Multiwfn 3.8 (dev) program. The orbital structures and NCIs of the monomers were visualized using the VMD 1.9.3 package.

Equation S1: Calculation of Na^+ diffusion coefficient (D_{Na^+})

$$D^{GIT} = \frac{4}{\pi\tau} \left(\frac{m_B V_M}{M_B S} \right)^2 \left(\frac{\Delta E_S}{\Delta E_\tau} \right)^2$$

where the pulse duration, mass of the active material (hard carbon), molar volume, molar mass, and V_M (mL mol⁻¹) are represented by the variables τ (s), m_B (g), molar mass, and M_B (g mol⁻¹). The area of electrode pole piece is S (cm²), the potential difference between two nearby steady states is ΔE_S , and the potential change brought about by the pulse current is ΔE_τ .

Equation S2: Calculation of activation energy for (de-)solvation by fitting the Arrhenius equation

$$\frac{1}{R_{ct/SEI}} = A \exp \left(-\frac{E_a}{RT} \right)$$

R_{ct} and R_{SEI} were obtained by fitting the impedance spectra of the electrodes at different temperatures (0-50°C), R is the ideal gas constant, A is the frequency factor.

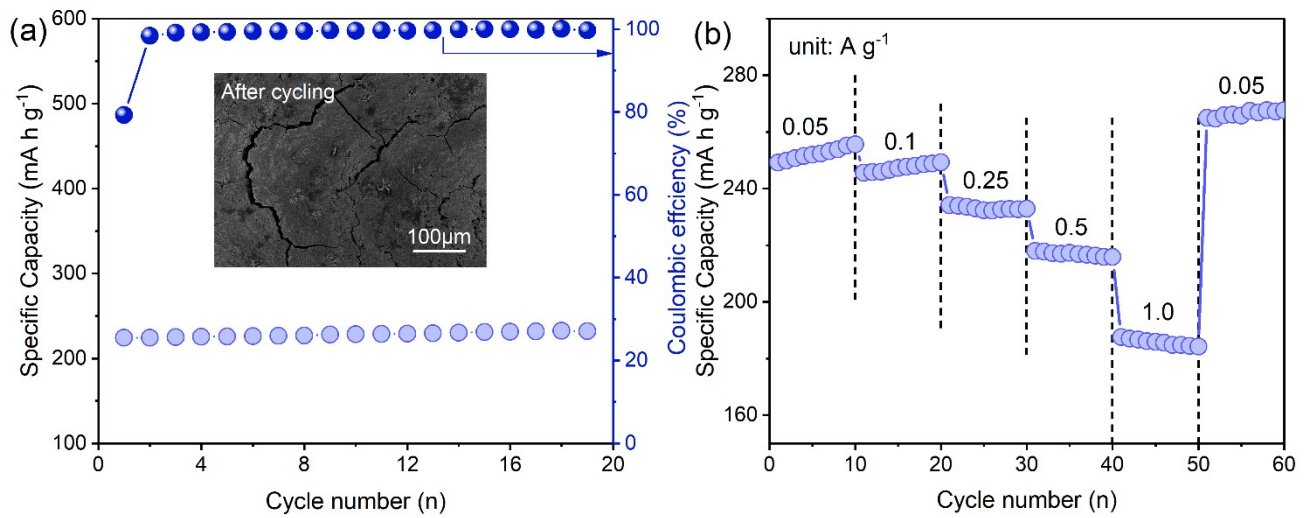


Fig.S1. (a) Cycling performance of HC-LS at 0.05A g^{-1} and SEM image of the electrode surface after cycling. (b) Rate performance of HC-LS at 0.05 to 1A g^{-1} .

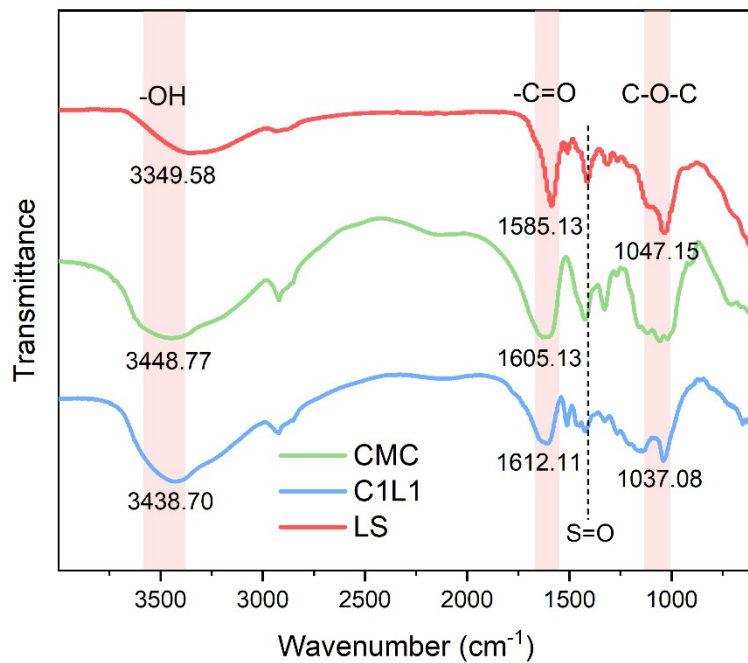


Fig.S2. FT-IR spectra of CMC, C1L1 and LS binders.

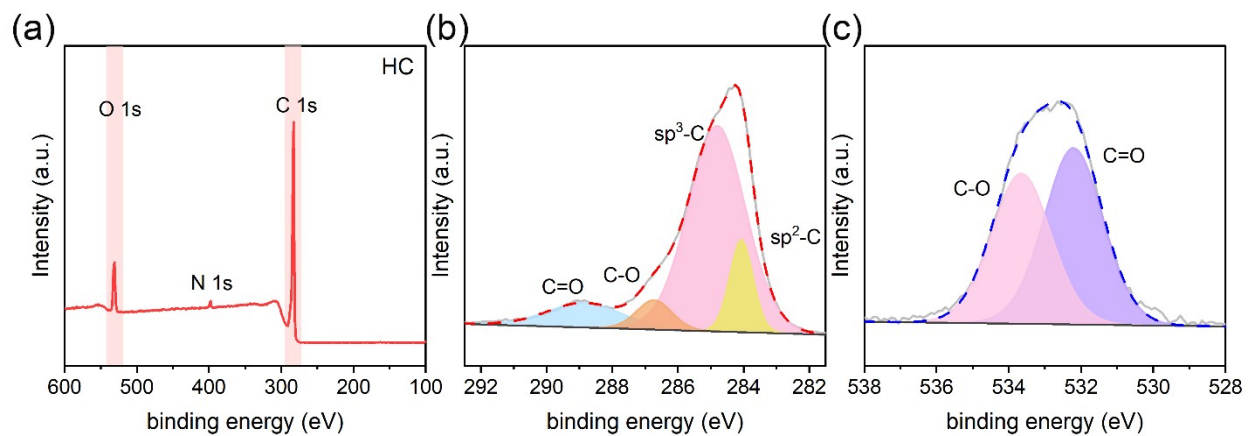


Fig.S3. (a) XPS survey scans of hard carbon. (b) C 1s of hard carbon. (c) O 1s of hard carbon.

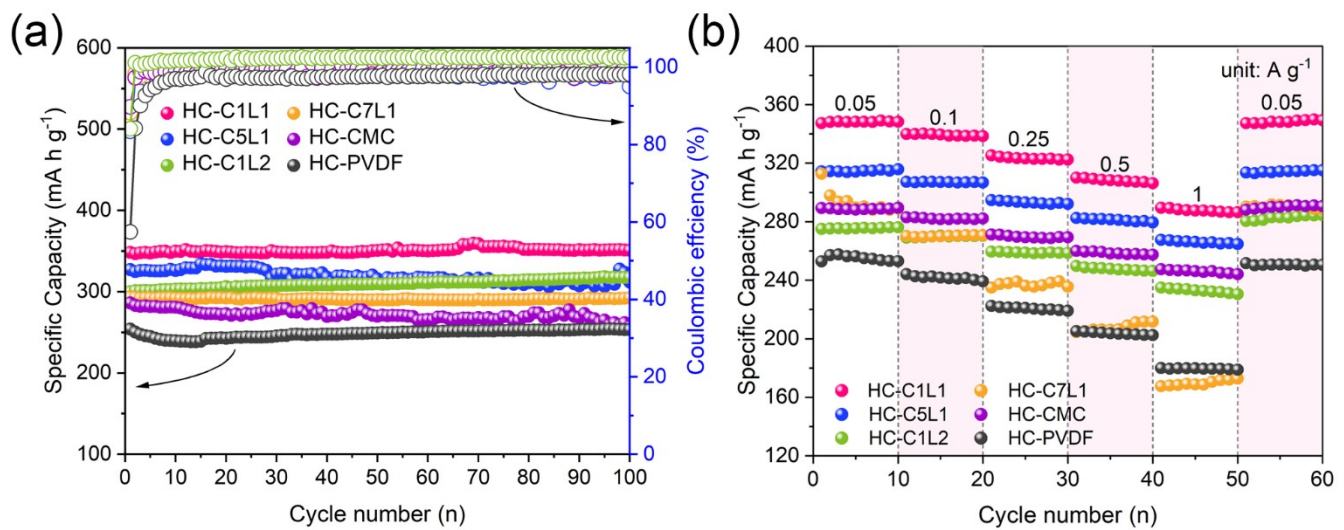


Fig.S4. Electrochemical performance of CMC/LS binders with different ratios. (a) cycling performance at 0.05 A g^{-1} current density, (b) rate performance.

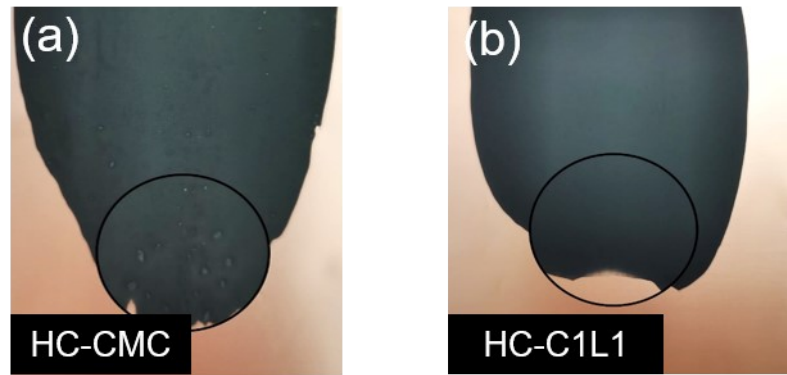


Fig.S5. Digital image of HC anode slurry on the collector after coating and drying. (a) HC-C1L1, (b) HC-CMC.

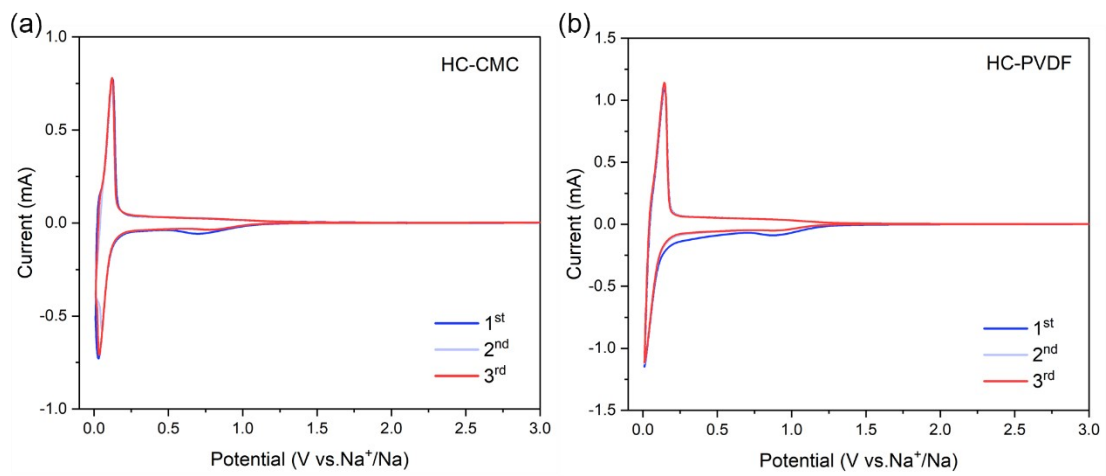


Fig.S6. CV curve of HC electrode at 0.1mV s^{-1} . (a) HC-CMC, (b) HC-PVDF.

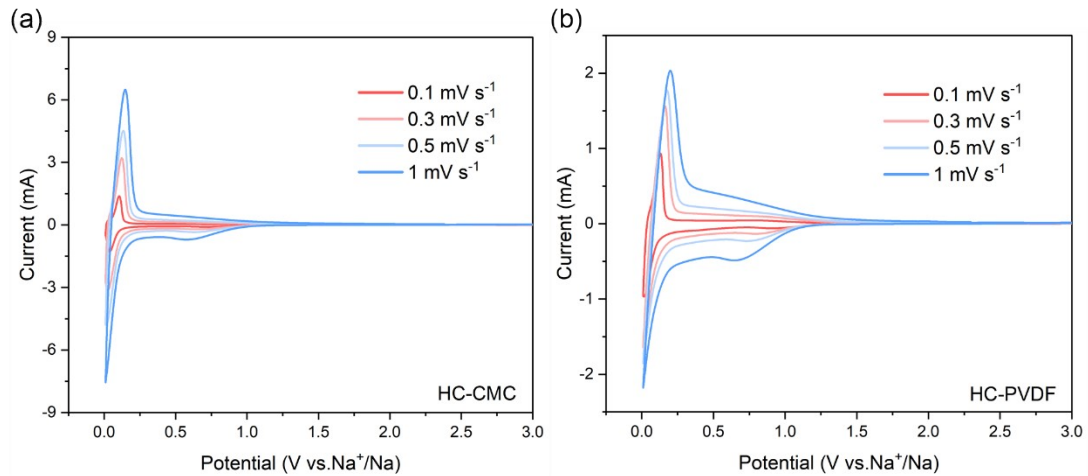


Fig.S7. CV curves of HC electrodes at different scan rates. (a) HC-CMC, (b) HC-PVDF.

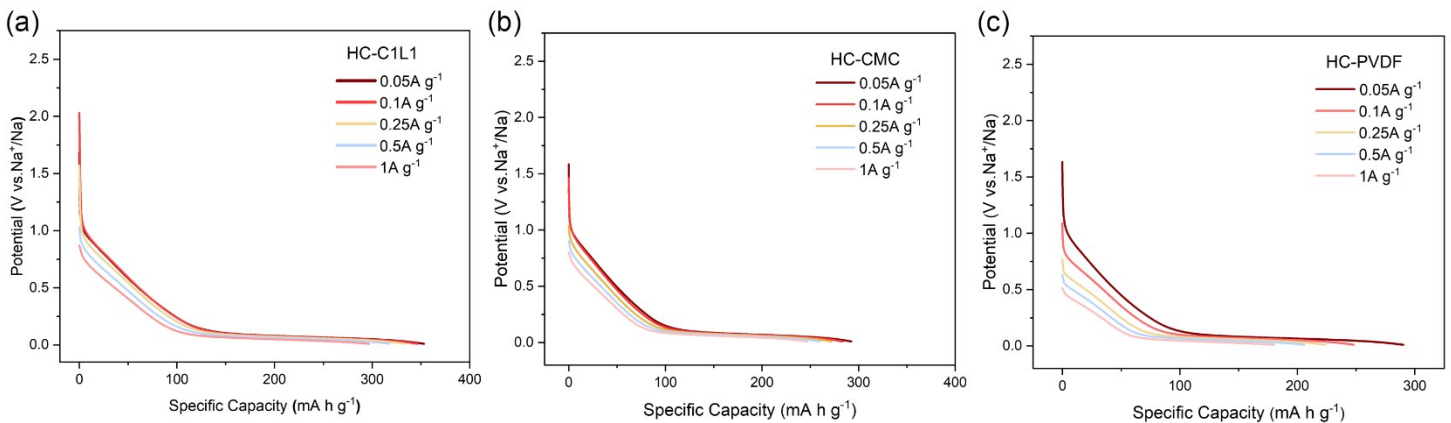


Fig.S8. Discharge curves (circle 2nd) of HC electrodes at different current densities ($0.05, 0.1, 0.25, 0.5$ and 1.0 A g^{-1}). (a)HC-C1L1, (b)HC-CMC, (c)HC-PVDF.

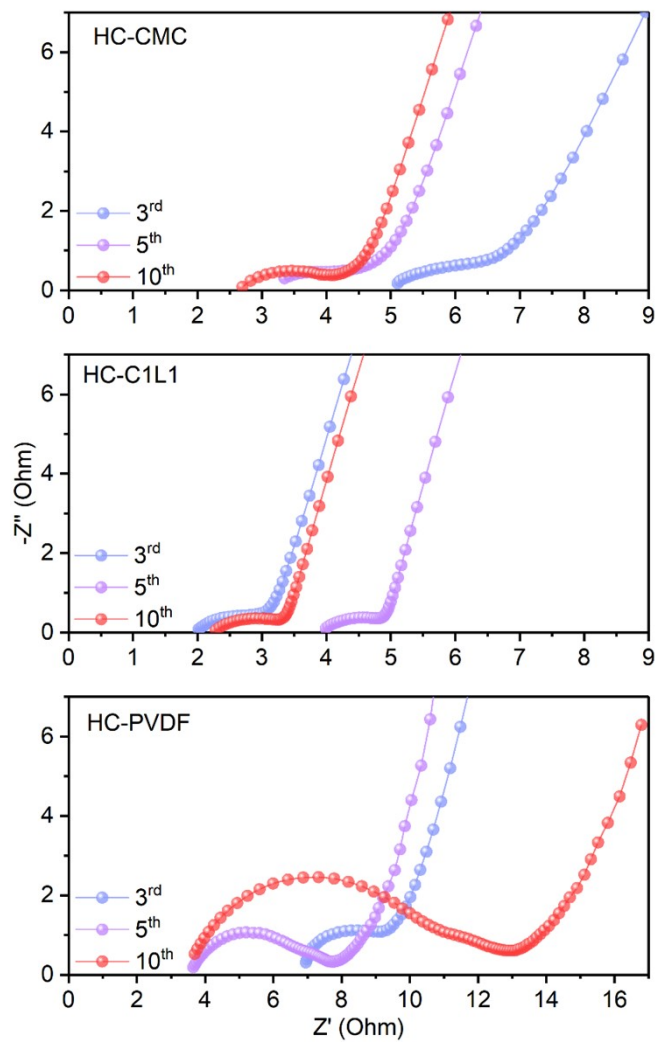


Fig.S9. Non-in situ EIS profiles of HC after 3 rd, 5 th and 10 th cycles.

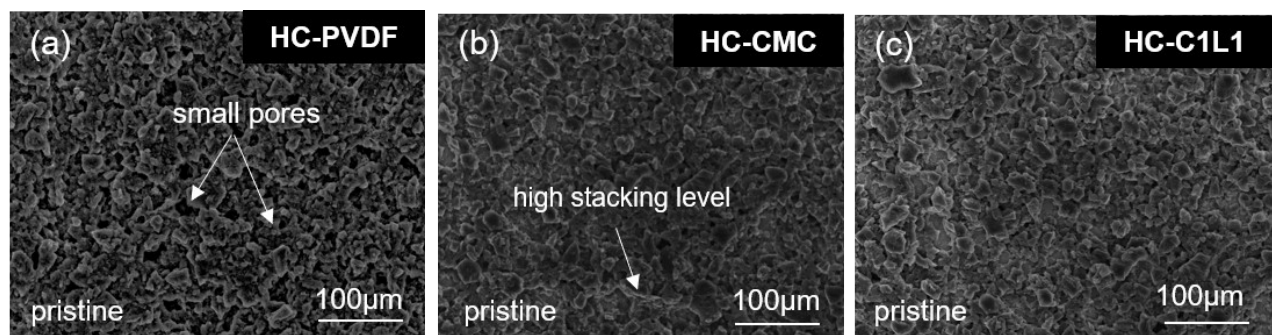


Fig.S10. SEM image of the HC electrode before cycling. (a) HC-PVDF, (b) HC-CMC, (c) HC-C1L1.

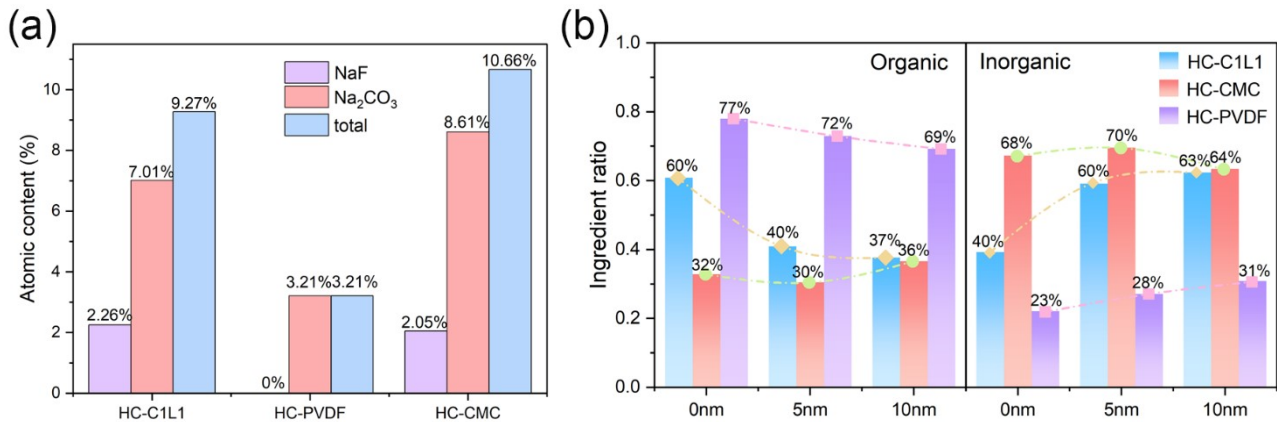


Fig.S11. (a) Peak area ration from inorganic component (Na-F and O-C=O peaks) of SEI layers derived from HC electrolytes before etching. (b) Plot of organic and inorganic compounds percentage evolution with etching depth for HC electrode.

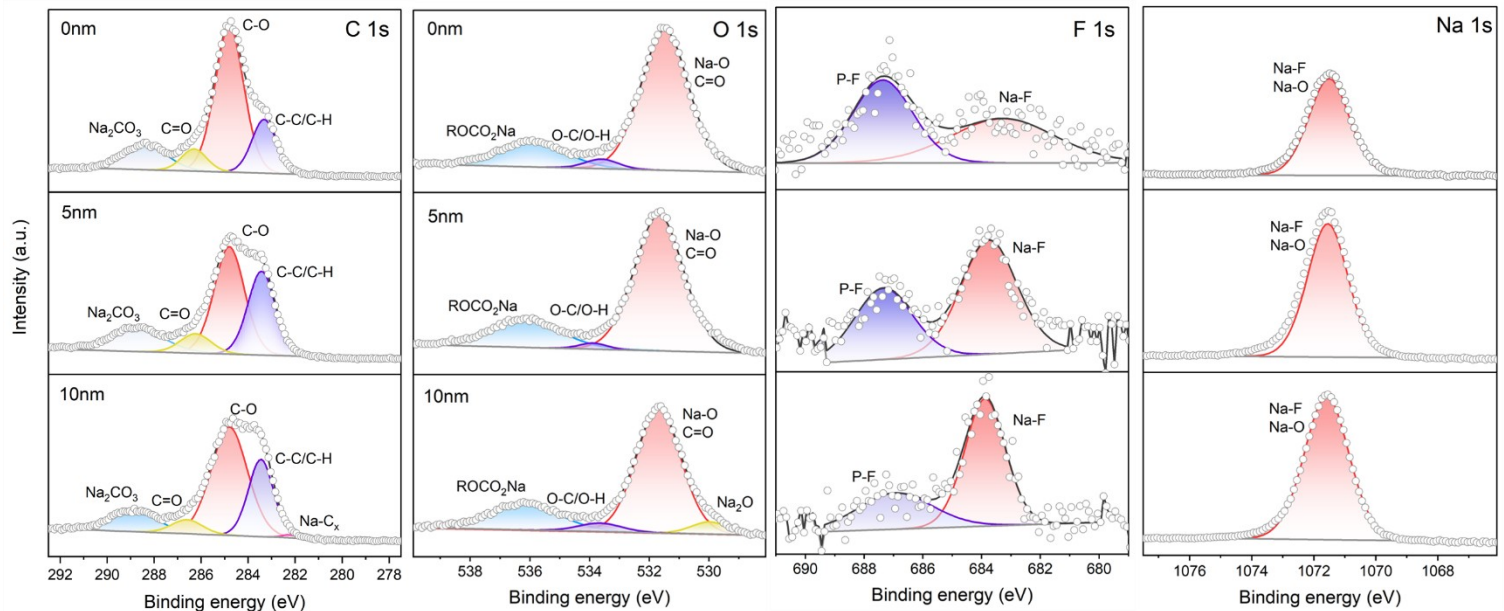


Fig.S12. XPS measurements of cyclic HC-CMC electrodes before and after performing Ar etching (0.05 A g⁻¹, 3rd cycle)

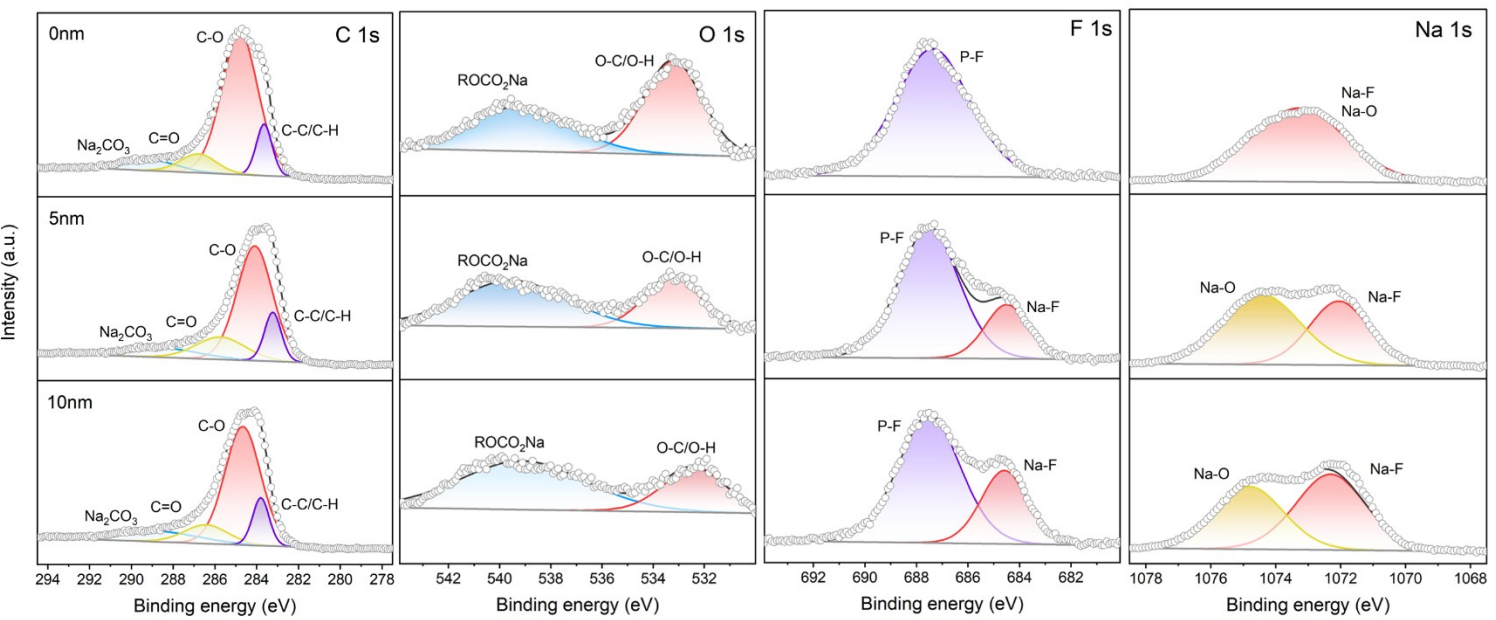


Fig.S13. XPS measurements of cyclic HC-PVDF electrodes before and after performing Ar etching (0.05 A g^{-1} , 3rd cycle).

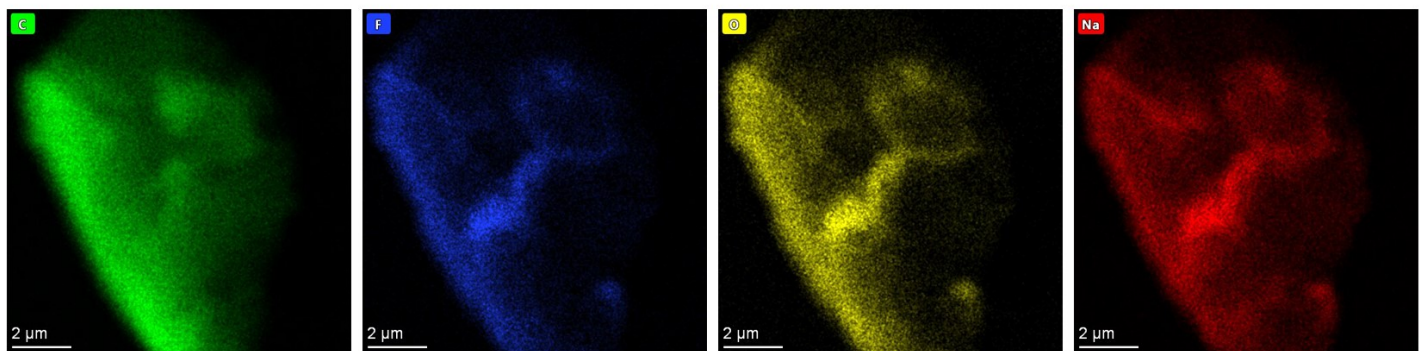


Fig.S14. EDX mapping of HC-CMC supplemented with elements.

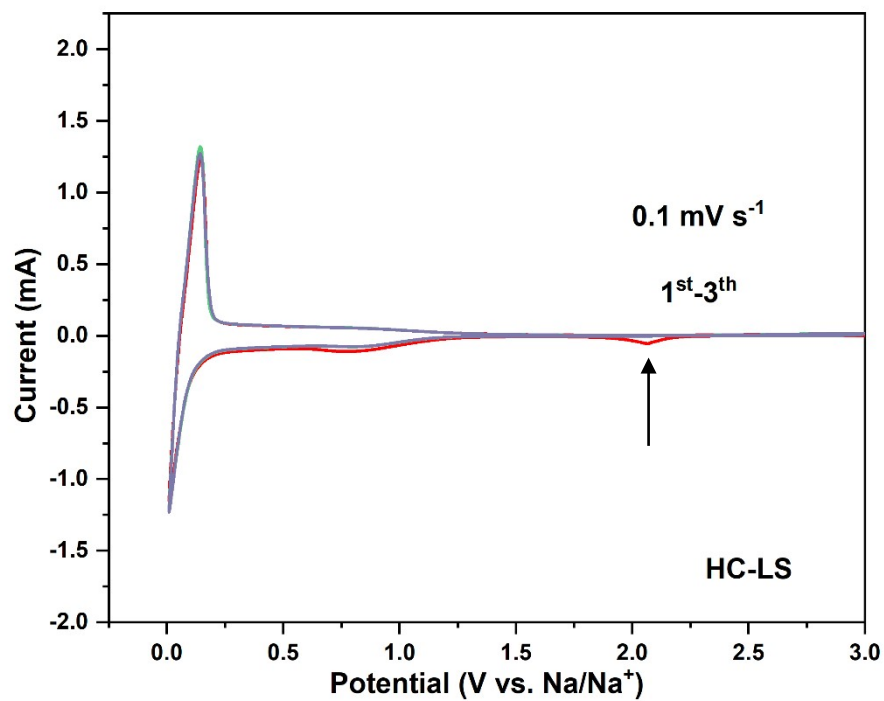


Fig.S15. CV curve of HC-LS (0.1 mV s^{-1}).

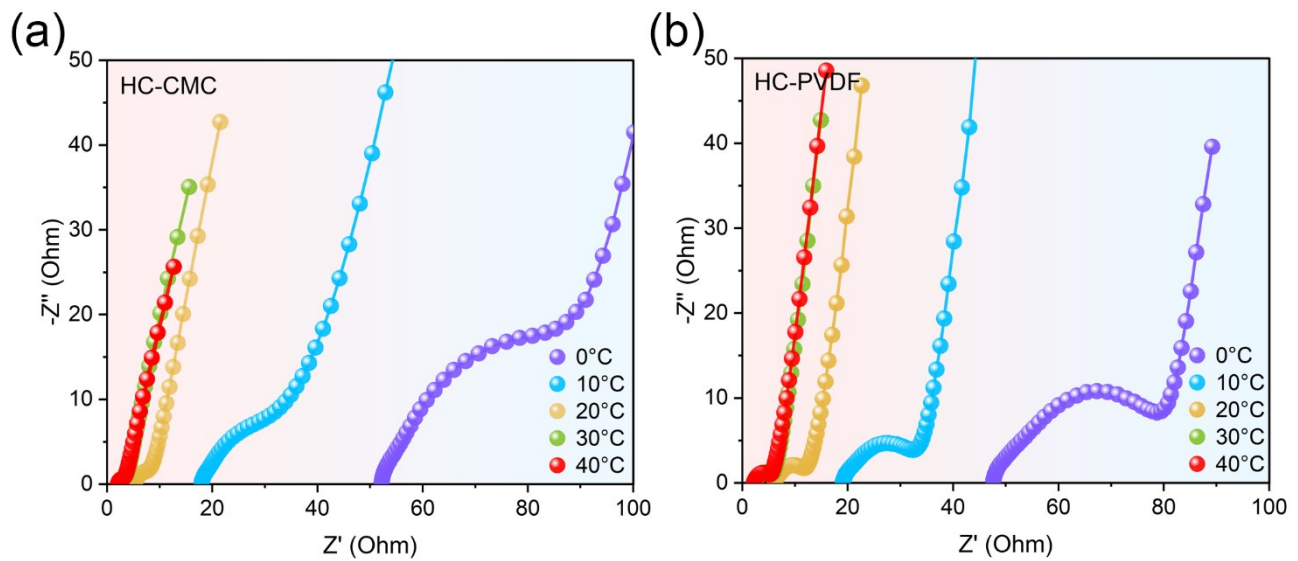


Fig.S16. Nyquist plots at different temperatures. (a) HC-CMC, (b) HC-PVDF.

Table S1. Parameters related to commercial hard carbon

electrode material	tap density (g cm ⁻³)	specific surface area (m ² g ⁻¹)
HC	0.77	3.58

Table S2. Carbon and oxygen bonding analysis of HC.

sample	Carbon bonding ratio (%)				Oxygen bonding ratio (%)	
	C=O	C-O	sp ³ -C	sp ² -C	C-O	C=O
HC	10.93	6.20	70.15	12.72	46.15	53.85

Table S3. A comparative analysis of the electrochemical characteristics of binders formulated with varying ratios of CMC and LS revealed notable distinctions.

samples	specific capacity (1 st cycle) (mAh g ⁻¹)	ICE (%)	capacity retention ratio (100 th cycle) (%)	Specific capacity (at 1 A g ⁻¹) (mAh g ⁻¹)
HC-C1L1	348.36	86.87	100.57	289.54
HC-C5L1	327.12	83.46	95.11	267.57
HC-C1L2	300.01	84.11	105.66	235.00
HC-C7L1	293.39	88.25	99.66	167.52

Table S4. Structural properties of HC-binders

samples	I _D /I _G	A _{D1} /A _G	A _{D4} /A _G
HC-C1L1	1.03	1.80	0.25
HC-CMC	1.05	1.88	1.04
HC-PVDF	1.11	1.81	0.58